A light-scattering study of 1-4 *cis* - *trans* polybutadiene

1997 J. Phys.: Condens. Matter 9 3803

(http://iopscience.iop.org/0953-8984/9/18/018)

J. Phys.: Condens. Matter **9** (1997) 3803–3820. Printed in the UK PII: S0953-8984(97)77699-9

A light-scattering study of 1-4 *cis–trans* polybutadiene

A Aouadi†, M J Lebon†, C Dreyfus†, B Strube‡, W Steffen‡, A Patkowski‡§ and R M Pick†

† LDMC, Université Pierre et Marie Curie, Tour 22 2ème-Casier 136, 4 Place Jussieu, 75252 Paris Cedex 05, France

‡ Max Planck-Institut für Polymerforschung, Ackermannweg 10, 55128 Mainz, Germany

§ Institute of Physics, A Mickiewicz University, Poznań, Poland

Received 9 September 1996, in final form 16 December 1996

Abstract. Light-scattering measurements on 1-4 polybutadiene of two molecular weights have been carried out using two different tandem Fabry–Pérot interferometers in the back-scattering and 90° scattering geometries. The Rayleigh–Brillouin spectrum has been measured at different temperatures through the glass transition. Relaxation times and sound velocities have been fitted to a hydrodynamic formula, with as few independent parameters as possible. Comparison with previous measurements shows that the Brillouin relaxation times do not follow the structural or α relaxation. Forcing the fit either with the times of the α process or with a high-frequency relaxation channel does not yield satisfactory results. The only processes arising on a similar timescale and with comparable activation energies are intra-chain conformational changes rates as computed by molecular dynamics. A possible mechanism linking these conformational changes to the damping of the Brillouin lines is suggested.

1. Introduction

Most of the recent experimental work on the liquid–glass transition in fragile liquids has been designed in order to test some of the predictions from recent theoretical developments of the physics of the liquid–glass transition [1]. These tests have, in fact, been focused primarily on the mode-coupling theory [2] which assumes that an (avoided) ergodic-to-non-ergodic transition takes place in the liquid phase, at a temperature T_c above the calorimetric glass transition, and predicts specific general dynamical features in the high-frequency domain. This theory, designed for spherical, interacting particles, has been tested by molecular dynamics simulations on model glass formers compatible with that pre-requisite [3] and it was found to reproduce correctly many of the numerical results. One of the theoretical predictions is that the viscosity has a strongly non-Arrhénius dependence [4], reminiscent of that which is found for real fragile liquids. Consequently, even though the latter are never formed of spherical molecules or ions, it is on such liquids that the comparison between theory and experiments has been performed. Such comparisons appear to have been successful in some specific cases. Yet, experimental proofs are still scarce and have often been spoiled by instrumental limitations or by spurious effects coming from the sample.

Some polymers are fragile glass-formers and can be cooled slowly from the melt or ‘rubbery state’ into the glassy state. Because of the technological importance of these polymers, their dynamical behaviour has been studied by several techniques and tested against glass transition theories, in spite of the intrinsic complexity of their structure. A

0953-8984/97/183803+18$19.50

peculiarity of many of these materials is the existence of secondary relaxations which still obscure the understanding of the glass transition [5]. Because side groups might be a very important origin of these extra relaxation mechanisms, the latter may be largely suppressed by selecting a side-group-free polymer, which explains the use of 1-4 polybutadiene as a prototype for these studies. The experiments also require that one eliminate any crystallization. This is achieved by selecting a polybutadiene formed of chains with an almost equal proportion of *cis* and *trans* monomers. Such a polymer has thus been studied by many techniques, among which are neutron diffraction and scattering experiments [6–14], dielectric absorption [15], NMR [16, 17], light-scattering experiments [18, 19] and simulation methods [20–22], each technique emphasizing some aspect of a relaxation process that is possibly related to the liquid–glass transition mechanism.

The present paper reports a Rayleigh–Brillouin scattering study performed in back-scattering and 90° scattering geometries on 1-4 polybutadiene of two different molecular weights. A short section describes the sample preparation and the experimental set-ups used in the present study. The experimental results are analysed in section 3 in terms of a relaxation mechanism which is compared with results obtained by some of the techniques mentioned in the previous paragraph. Our analysis does not confirm the items of evidence previously proposed [7–10] to support a mode-coupling theory (MCT) description of the liquid–glass transition in polybutadiene (PB). Furthermore, our experimental data obtained form depolarized light scattering (DLS), which are also reported and discussed in section 3, cannot be described in terms of relaxation times obtained on a large temperature scale by other techniques. In section 4 we propose that this apparent discrepancy is due to the fact that Brillouin scattering mainly couples to a relaxation mechanism which has been revealed by molecular dynamics techniques [21] but which might not be detected by other techniques.

2. Materials and methods

2.1. Materials

Two 1-4 poly-butadiene samples were synthesized by anionic polymerization as described in [23]. The molecular weights of our samples were determined to be $M_w = 7675$ and $M_w = 20\,000$, both of which were below the entanglement molecular weight with a polydispersity $M_w/M_n = 1.05$ (measured by gel permeation chromatography (GPC)). Their glass-transition temperatures were measured by 10 K min^{-1} differential scanning calorimetry (DSC) to be 176 and 175 K, respectively. No sign of crystallization was found in the DSC curves, as expected for such a random co-polymer consisting of *cis*, *trans* and *vinyl* repeat units in the ratio 46:47:7, as deduced from ^{1}H NMR (300 MHz). In order to eliminate any light-scattering channel not related to polybutadiene, the samples were kept free from any stabilizer. To prevent cross linking of the polymer, our samples were stored in the dark at $-20\,^\circ$C between experiments and no experiments were performed above 50 °C. The absence of such cross linking was checked through various GPC measurements performed at different stages of the sample preparation and after the light-scattering measurements.

All impurities such as dust and water were removed by dissolving the polybutadiene in benzene, drying the solution for several days over a molecular sieve and filtering it, through a 0.22 μm Millipore filter, directly into the dust-free light-scattering cells which were in the form of Pyrex cylindrical tubes of 10 mm inner diameter. A final freeze drying of the sample removed the solvent before the cell was flame sealed under vacuum. The content of benzene in the sample was controlled by monitoring the intensity of the very strong 991 cm^{-1} ring-breathing A_{1g} vibration of the benzene ring by Raman scattering [24]. The

absence of any detectable peak at that frequency was a good indicator of the absence of benzene as solvent.

2.2. Light-scattering measurements

Two independent experiments were performed: (i) in Paris the PB of $M_w = 7675$ was measured in the range 150–325 K in a near-back-scattering geometry (175°) with an eight-pass (four plus four) tandem Fabry–Pérot interferometer (TFPI) [25] and an Ar^+ ion laser (Coherent) emitting at 514.5 nm; and (ii) in Mainz the PB of $M_w = 20\,000$ was measured in the temperature range 210–295 K at a scattering angle of 90° using a six-pass tandem Fabry–Pérot interferometer (JRS, Affoltern, Switzerland) and an Ar^+-ion laser (Spectra Physica) ($\lambda = 514.5$ nm) [26]. The scattering cell was mounted in a cryostat with temperature stability within 0.25 K and, for reasons explained above, no experiment was performed above 325 K. An example of the spectra obtained in v–(v + h), v–v and v–h back-scattering geometries is shown in figure 1. Even at the highest temperature used, the shapes and intensities of v–(v + h) and v–v spectra were quite similar, the v–h intensity I_{VH}, which is equal to the so-called anisotropic intensity [27], being about one order of magnitude less intense. Consequently, the contribution of the anisotropic intensity to the v–v spectra could be and was always neglected in the analysis of the Brillouin profiles. Additionally, the depolarized light-scattering spectra were recorded with the TFPI for five different free spectral ranges [25] and, at higher frequencies, with a double-grating Raman spectrometer [26] (SPEX 1403, 1800 lines/mm, focus 850 mm) so that composite spectra [28] were obtained between 1 GHz and 4 THz for five temperatures.

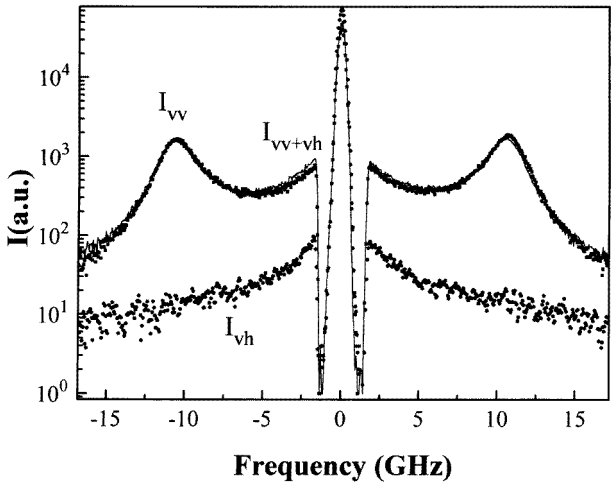

Figure 1. A comparison of v–v plus v–h (——), v–v (■) and v–h (●) spectra (respectively I_{vv+vh}, I_{vv} and I_{vh}) measured in the back-scattering geometry at 293 K.

The temperature variation of the shift in the Brillouin line frequency ω_B and of its width (HWHM), $\Delta\omega_B$, are shown in figures 2(a) and (b) for the scattering angles of 175° and 90°, respectively. Also shown in figures 2(a) and (b) is the frequency $\omega_0 = C_0 q$, where q is the scattering wavevector of the Brillouin experiment and C_0 is the velocity of sound at low frequency, which was obtained from ultrasonic measurements performed by a transmission method at 5 MHz. C_0 was found to vary linearly in the range 235–300 K and may be

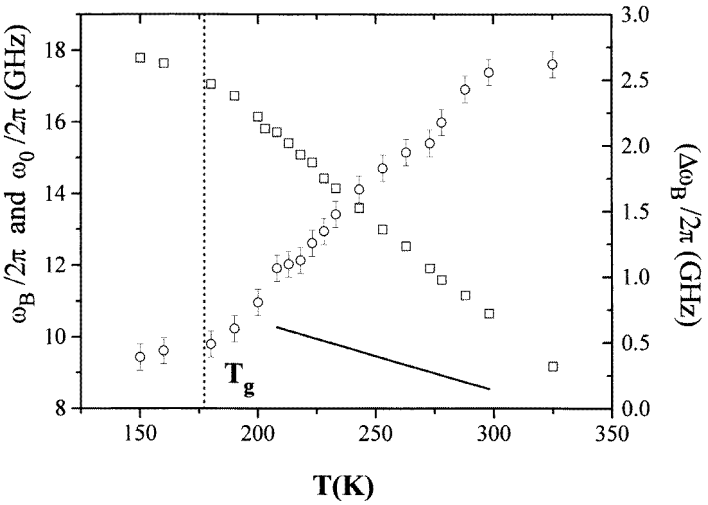

Figure 2. The frequencies ω_B (□) and widths $\Delta\omega_B$ (○) of Brillouin lines obtained from the measurements at scattering angles of (a) 175°, and (b) 90° with frequency $\omega_0 = C_0 q/(2\pi)$ (——) from acoustic measurements.

expressed as

$$C_0(T) = (1537 - 3.28T(^\circ\mathrm{C}))\ \mathrm{m\ s^{-1}} \tag{1}$$

This formula is in very good agreement with a previous measurement [18] by Fioretto *et al* on a film of polybutadiene of high relative molecular weight.

Two aspects of our results, seen respectively in the v–v spectrum in figures 1 and 2 must be pointed out: (i) Even at the highest temperature at which we performed measurements, ω_0 and ω_B had quite different values. This is in line with the fact that the Brillouin line width $\Delta\omega_B$ increases over the whole temperature range investigated, contrary to the usual behaviour in viscoelastic fluids, namely that at sufficiently high temperatures, the width begins to decrease. Indeed, this continuous increase implies that, assuming that a mean relaxation time $\langle\tau\rangle$ characterizes the relaxation processes to which the longitudinal phonons couple, the temperature at which the condition $\langle\tau\rangle\omega_B = 1$ is fulfilled has not yet been reached at 325 K. (ii) As central peak is clearly visible in figure 1 and we checked that this low-frequency increase in the intensity was not related to the wings of the elastic Rayleigh line. The depolarization ratio was found to be equal to 0.74 far above the Brillouin line. Within the frequency range near and below the Brillouin line the experimentally measured anisotropic contribution to the v–v spectra was negligible. This low-frequency contribution is thus a part of the whole relaxation process, so these two aspects will have to be taken into account in the analysis of the v–v spectra.

3. Results and discussion

The analysis of the Brillouin triplet was performed using the following expression for the intensity [29]:

$$I(\omega) = \frac{I_0}{\omega}\,\mathrm{Im}[\omega_0^2 - \omega^2 - \mathrm{i}\omega\gamma_0 - \omega m(\omega)]^{-1} + I_{BG} \tag{2}$$

where I_0 is a normalization constant, I_{BG} is the background intensity, $\omega_0 = C_0 q$, the frequency of acoustic waves at zero frequency, C_0, the velocity of sound and q, the wavevector of the experiment. The entire physics is thus represented by the constant γ_0 and the relaxation function $m(\omega)$.

3.1. The hydrodynamic analysis

3.1.1. Parameters. In this first analysis of the low-frequency isotropic spectra, γ_0 was taken as a temperature-independent linewidth which was expected to represent all the anharmonic processes still present at low temperature, while $m(\omega)$ was supposed to describe the relaxational processes to which the longitudinal phonons couple. In such an analysis, $m(\omega)$ is usually taken as an empirical function, several forms for which have been given in the literature [30–32]. In the following analysis, which has already been performed on several glass-forming liquids [18, 29, 33, 34], we took a Cole–Davidson function for the relaxation function $m(\omega)$:

$$m(\omega) = \frac{\Delta^2}{\omega}[(1 - \mathrm{i}\omega\tau_{CD})^{-\beta_{CD}} - 1]. \tag{3}$$

The analysis of the whole spectrum involves seven parameters. Allowing all of them to vary would result in large ambiguities in their values. Therefore, the fit was performed under the following constraints.

(i) According to a previous analysis [29], γ_0 was assumed to be the sole contribution to the line width below the glass temperature ($T_g = 176$ K) at 165 K and was measured directly at that temperature as $\gamma_0 = 0.2$ GHz. We assume that the relative contribution of the very high-frequency parts of the spectrum taken care of by γ_0 can be taken to be constant with temperature to keep the fit as simple as possible and in order not to introduce another fitting parameter. For reasons indicated in section 3.1.2, a second analysis was performed keeping $\gamma_0 = 0$.

(ii) ω_0 was computed from equation (1) using $\omega_0 = C_0 q$ and we assumed that this equation, which had been checked to be valid down to 235 K, could be extrapolated throughout the range 235–150 K.

(iii) The parameter β_{CD} was taken from neutron spin echo (NSE) experiment [9] at wavevector $q_0 = 1.48$ Å^{-1}, corresponding to the maximum of the static structure factor, and is thought to describe the α relaxation process. In [9], the relaxation function was taken as a Kohlrausch function ($\tau_{KWW} = \alpha \exp[-(t/\tau)^{\beta_{KWW}}]$) and the parameter $\beta_{KWW} = 0.45$ was found to be constant throughout the temperature range. Our β_{CD} parameter was obtained by making use of the correspondence between the parameters of the Kohlrausch and of the Cole–Davidson laws given in [31], which yielded $\beta_{CD} = 0.31$.

(iv) The parameter Δ is connected to ω_∞ by the usual equation $\omega_\infty^2 = (C_\infty(T)q)^2 = \Delta^2 + \omega_0^2$.

The fits for the experimental data measured in the back-scattering mode are shown for different temperatures in figures 3(a)–(c). Values of the parameters not fixed above are given in table 1, together with the confidence parameter χ^2 of the fit. The agreement throughout the frequency range and the low value of χ^2 for all temperatures show that the hydrodynamic formulation proposed above describes the experimental data quite satisfactorily, in particular concerning the spectral features mentioned above. This fitting procedure will be referred to as fit 1 henceforth. Corresponding fits to the experimental data measured at the scattering angle of 90° are shown in figure 3(d). In these fits parameters from table 1, corrected for the scattering angle, were used and are given in table 2.

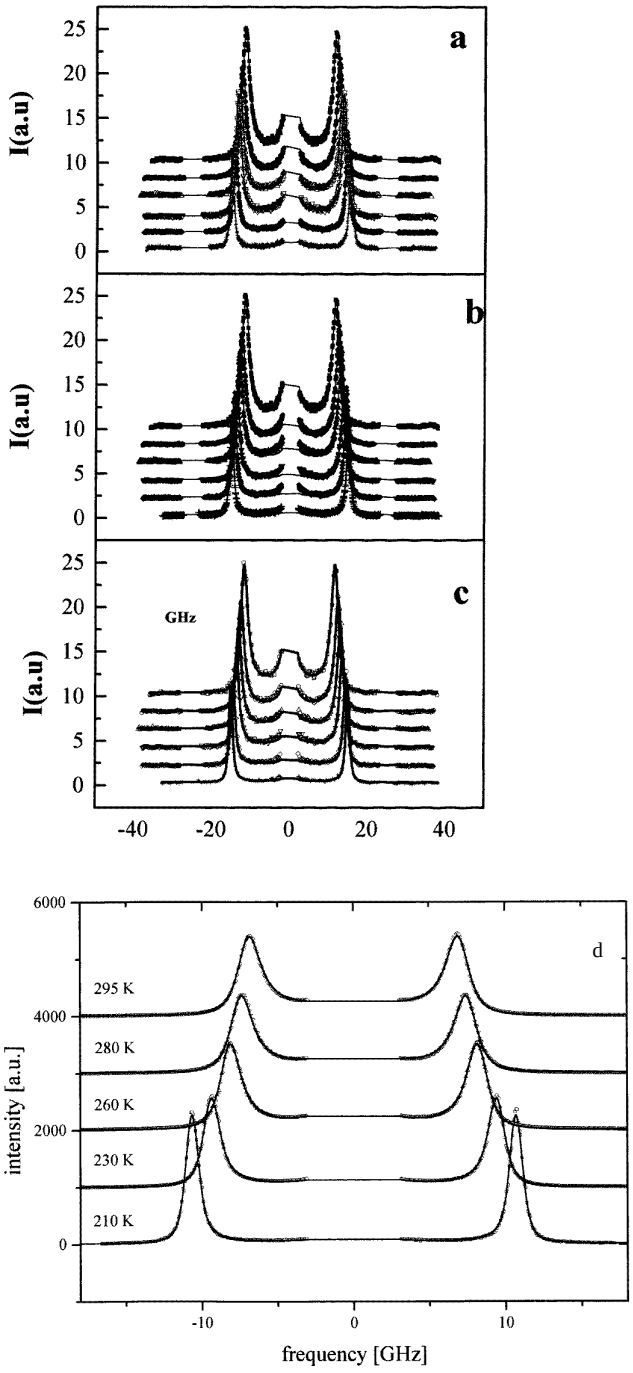

Figure 3. The thermal variation of the Brillouin spectra shown together with fits using equation (2) for back scattering, at temperatures of 278 K (■), 263 K (●), 253 K (△), 243 K (▽), 228 K (♦) and 233 K (+). (a) In fit 1 β and γ_0 are fixed, τ is free. (b) In fit 2 τ is fixed from NSE relaxation times [10] at $q = 1.88$ and β is fixed, γ_0 is free. (c) In fit 3 τ is as in fit 2 and γ_0 is fixed, β is free. In (d) 90° scattering at temperatures of 210, 230, 260, 280 and 295 K is shown.

Table 1. Fitting parameters and variables for back-scattering geometry: ω_B measured directly from the spectra, ω_0 obtained from ultrasonic measurements and γ_0 obtained from the width of the Brillouin lines measured at low temperature. Δ and τ_K were obtained from the fit. The Kohlrausch time was obtained using the correspondence [31] between τ_{CD} and τ_K, namely $\tau_K = \tau_{CD}(1.184\beta_{CD} - 0.184)$. f_0 is the non-ergodicity parameter; χ^2 gives the confidence in the fit.

T (K)	$\omega_B/(2\pi)$ (GHz)	$\omega_0/(2\pi)$ (GHz)	$\Delta/(2\pi)$ (GHz)	$\omega_\infty/(2\pi)$ (GHz)	τ_K (ns)	f_0	χ^2
325	9.17	8.02	8.60	11.76	0.007	0.53	1.92
314	9.60	8.23	8.95	12.16	0.010	0.54	1.08
298	10.66	8.54	9.23	12.58	0.012	0.54	1.84
294	10.71	8.61	9.32	12.69	0.014	0.54	1.39
288	11.16	8.73	9.71	13.06	0.018	0.55	1.25
278	11.60	8.92	10.08	13.47	0.023	0.56	1.33
273	11.92	9.02	10.19	13.61	0.029	0.56	1.49
263	12.53	9.21	10.62	13.92	0.048	0.57	1.06
253	13.00	9.40	10.94	14.42	0.063	0.57	1.99
243	13.60	9.59	11.31	14.83	0.097	0.58	1.80
233	14.15	9.78	11.60	15.17	0.169	0.58	1.81
228	14.43	9.88	11.77	15.37	0.224	0.58	1.63
223	14.87	9.98	11.92	15.54	0.450	0.59	1.57
218	15.09	10.07	12.11	15.75	0.501	0.59	1.74
213	15.41	10.17	12.31	15.96	0.630	0.59	1.48
208	15.72	10.26	12.67	16.31	0.645	0.60	0.98
200	16.15	10.42	13.02	16.68	1.749	0.60	1.18
190	16.73	10.61	13.56	17.22	3.019	0.62	1.91
180	17.05	10.80	13.72	17.46	5.495	0.62	1.65
170	17.27	10.99	13.70	17.57	13.803	0.61	3.71
160	17.46	11.18	13.73	17.70	15.135	0.60	1.85
150	17.78	11.38	13.97	18.01	32.359	0.60	1.85

Table 2. Fitting parameters and variables for 90° scattering geometry. See table 1 for explanation of symbols.

T (K)	$\omega_B/(2\pi)$ (GHz)	$\omega_0/(2\pi)$ (GHz)	$\Delta/(2\pi)$ (GHz)	τ_K (ns)	χ^2
294	6.53	6.14	6.08	0.01	3.19
280	7.06	6.28	6.29	0.014	3.06
260	7.83	6.56	6.92	0.036	2.15
230	9.08	6.95	7.57	0.21	3.57
200	10.36	7.37	8.47	0.66	2.32

3.1.2. Discussion of the results. Figure 4 shows the variation of the velocity of sound at infinite frequency C_∞ and of the non-ergodicity parameter [35]:

$$f(T) = 1 - C_0^2(T)/C_\infty^2(T). \tag{4}$$

C_∞ varies smoothly with decreasing temperature and seems to approach $C_B = \omega_B/q$ only in the vicinity of the glass-transition temperature. This is quite different from other systems, such as salol [33] for example, for which the curves of the two velocities depart one from the other only well above the glass-transition temperature: in such cases, the relaxation time associated with the relaxation processes becomes much longer than the Brillouin period well above T_g, whereas the situation is certainly different in polybutadiene.

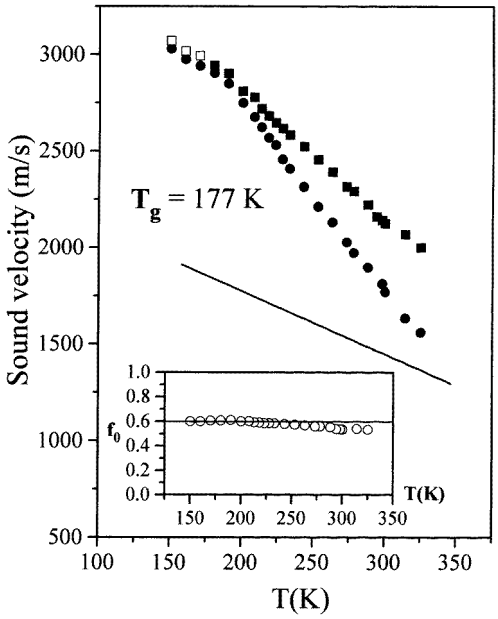

Figure 4. The temperature behaviour of the velocities of sound of: C_B (●), the velocity of sound computed from the maximum of the Brillouin lines; C_0 (——), that from acoustic measurements and extrapolation at lower temperature; and C_∞ (■), that from the fit using equation (2); the points (□) are from the fit taking $\gamma_0 = 0$. The temperature dependence of the non-ergodicity parameter $f_0(T) = 1 - (C_0(T)/C_\infty(T))^2$ is shown in the inset (○).

We also find that, around T_g, $C_\infty(T)$ has a marked change of slope, which effect is found for all glasses [36] and has a purely thermodynamic origin, namely the freezing in of the structure at T_g, which is of no interest here for further discussion. Contrary to the NSE results [9] and as in a previous Brillouin study [18], we do not find a cusp in the non-ergodicity parameter $f_0(T)$. The absence of this cusp, both in $C_\infty(T)$ and in $f(T)$, above T_g, does not in itself exclude the possibility that MCT applies to polybutadiene, because $C_\infty(T)$ of equation (4) must be understood as the velocity of sound at a frequency much above the structural relaxation frequency and, simultaneously, in a frequency domain in which no other relaxation phenomenon has any appreciable spectral weight. We shall see below that this is certainly not the case here, so that our experimentally determined $C_\infty(T)$ is not the quantity to which MCT refers [35]. The most that we can say is that our results do not exhibit the cusp predicted by idealized MCT.

Another and quite different problem arises when one compares the relaxation times in table 1 with those obtained by different authors and/or techniques. Figure 5 reports

(i) the Kohlrausch relaxation times obtained from the back-scattering experiments the error bars corresponding to different values for γ_0 (see below);

(ii) the corresponding times obtained for the 90° scattering Brillouin experiment; and

(iii) the relaxation times from the Brillouin experiment of Fioretto *et al* [18], performed on a *cis–trans* PB film.

Although these three Brillouin results were obtained on polybutadienes having different molecular weights and sample preparations (film or bulk) and even though the methods for treating the experimental data show some differences, the corresponding relaxation times

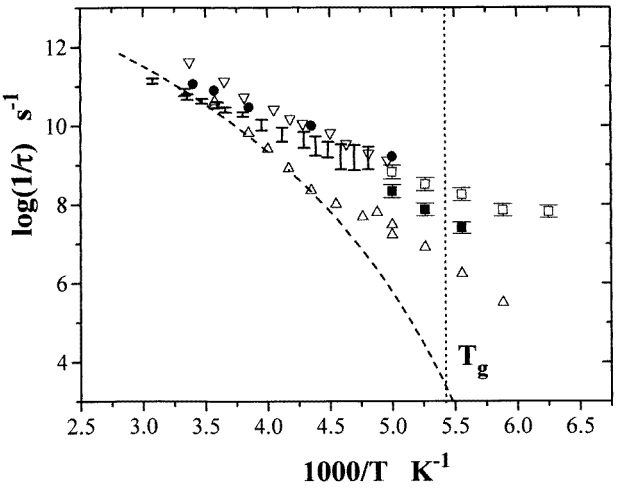

Figure 5. An activation plot showing Kohlrausch relaxation times versus the inverse of the temperature: (■) and (□), Brillouin light scattering (back-scattering geometry) for $\gamma_0 = 0$ and 0.2 respectively, (I) joins the Kohlrausch relaxation times obtained through the two fits and is taken to be experimental error; (●), Brillouin light scattering (90° geometry); (▽), Brillouin light scattering from a PB film [18], (△), NSE data [10] for $q = 1.88$ Å^{-1}; and (– – –), the Rouse model [7, 10] for $q = 1.88$ Å^{-1}.

are similar, except at the highest temperatures. On decreasing temperature, all depart very rapidly from the relaxation time which scales with viscosity [9, 10, 15]. This departure is far beyond our experimental margin of error: indeed, we obtain τ_{KWW} through a fit of the entire v–v spectrum which has a low-frequency cut-off at approximately $\nu_c = 1$ GHz (while the Brillouin frequency is approximately at 10 GHz). τ_{KWW} will suffer from large uncertainties only when $\langle\tau_{KWW}\rangle^{-1} < \nu_c$ (where $\langle\tau_{KWW}\rangle = (1/\beta_{KWW})\Gamma(1/\beta_{KWW})\tau_{KWW}$). Assuming that τ_{KWW} will be properly determined for shorter relaxation times, namely for $\tau_{KWW} < 10^{-9}$ s, the quasi-linear aspect of $\log(\tau_{KWW})$ as a function of T^{-1} shown in figure 5 indicates that, even for longer relaxation times, our estimate of τ_{KWW}, even though it is less precise, nevertheless shows the correct trend. These times do depart more and more from the values obtained in the Rouse model [9], when T^{-1} increases. Our measurements seem thus to reveal a relaxation time different from the α relaxation time, defined here as the Rouse model time. The same result of fits to Brillouin data with Cole–Davidson or Kohlrausch functions producing relaxation times far below those form other measurements has been found previously in other materials [37].

The model (equations (2) and (3)) used in the above analysis is nevertheless not fully consistent because, even though we took γ_0 as the intrinsic Brillouin linewidth at T_g, it appears that this linewidth still decreases noticeably below T_g. To check that this extra thermal variation in $\gamma_0(T)$ was not the reason of the strong departure of the Brillouin τ_{KWW} from the α process, we performed another fit of our entire data set taking $\gamma_0 = 0$. The error bars shown in figure 5 represent the differences between the values obtained for τ_{KWW} in those two fits. They show that, at least above 220 K, the value of γ_0 has little influence on the order of magnitude of the Brillouin τ_{KWW}.

3.1.3. A comparison with other relaxation times. Several other experimental techniques have been used to determine these relaxation times for different polybutadienes or related substances. These techniques were dielectric relaxation [15], fluorescence anisotropy decay [38], ^{13}C NMR [16], photon correlation spectroscopy (PCS) [24] and spin-echo ^{2}H NMR [17]. Most of the dielectric, spin-echo ^{2}H NMR and PCS experiments were performed on polybutadienes of similar chemical structure though different molecular weights. Conversely, the ^{13}C NMR data were obtained for an almost pure *cis*-polybutadiene ($M_W = 320\,000$, $T_g = 161$ K), a structural change which can affect the comparison to some extent.

In these different sets of data, shown in figure 6, the relaxation times clearly scale with a relaxation time [10] derived from the viscosity of polymer blends via the Rouse model [9], so that all these techniques measure the α relaxation. Yet, the dielectric measurements reveal the existence of another relaxation time, a β relaxation [15], which separates from the α relaxation process at around 200 K, 20 K above T_g, showing an Arrhénius temperature dependence characterized by an activation energy of 9.5 kcal mol^{-1}. Interestingly enough, the NSE relaxation times measured by Richter *et al* [10], who performed their experiment at $q = 1.88$ Å^{-1} at the first minimum of the static structure factor, revealed the same type of phenomenon but displaced on frequency and temperature scales: below $T = 220$ K, the NSE relaxation times show an Arrhénius behaviour with approximately the same activation energy as that of dielectric ones but they are more than two orders of magnitude shorter at the same temperature [14]. The NSE relaxation times become equal to the α relaxation time at around 220 K and, above that temperature, they follow the Rouse curve (see figure 6). Richter *et al* pointed out that the change in regime at around 220 K coincides with the critical temperature T_c proposed in a MCT analysis of the non-ergodicity factor in [9].

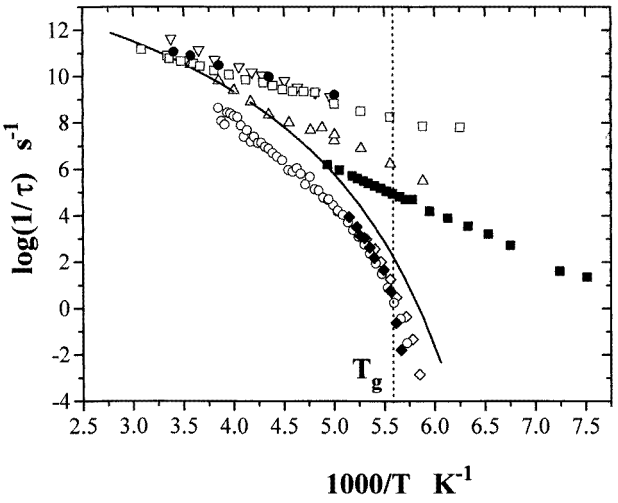

Figure 6. An activation plot showing Kohlrausch relaxation times versus the inverse of the temperature as in figure 5 but with (○) and (■), dielectric measurements [15] for α and β relaxations respectively; (◊), photon correlation spectroscopy [24], and (♦), the spin–lattice relaxation time of ^{1}H from NMR spectroscopy [17].

Actually, the τ_{KWW} values obtained in our analysis still follow the Arrhénius behaviour, but they are again one to two orders of magnitude shorter than the NSE ones. They then join the α relaxation times at around $T = 285$ K and the temperature domain within which

those times are comparable is too small to decide whether the Brillouin τ_{KWW} values and the α relaxation times really differ from one another above that temperature. Within the constraints of the fitting procedure, however, the activation energy is smaller. In fact, this activation energy is not a well-defined quantity because its value depends on the choice we made for the value of the coefficient β_{KWW} (the higher β_{KWW} the lower the corresponding activation energy). By choosing $\beta_{KWW} = 0.45$, namely the value found in the analysis of the $q = 1.48$ Å^{-1} NSE experiment and associated with the α relaxation, one deduces an activation energy of 5 kcal mol^{-1}, half the activation energy of the relaxation process which couples to this short-wavelength, local dynamics. Taking $\beta_{KWW} = 0.37$, a value found in the analysis of the $q = 1.88$ Å^{-1} NSE experiment [10] and associated with the β relaxation, yields a similar discrepancy in relaxation times and an activation energy equal to 6.3 kcal mol^{-1}. In other words, the comparison of the Brillouin, NSE and dielectric data suggests that there could exist a general relaxation phenomenon characterized by a broad distribution of relaxation times, each particular technique coupling strongly to some specific part of the distribution, whence yielding specific relaxation times. Such a description is not contradictory to our low-temperature data, because we already pointed out that our Brillouin linewidth still decreases smoothly below T_g (this was our motivation for a second fit with $\gamma_0 = 0$, keeping for $m(\omega)$ the expression by equation (3)). The comparison with the NSE and dielectric data suggests that the hypothesis made for choosing γ_0 and $m(\omega)$ may have been inappropriate and that we should first consider whether we can find some other indication of a broad relaxation phenomenon.

3.2. Depolarized light-scattering measurements and comparison with NSE data

The depolarized light-scattering (DLS) spectra, measured as described in section 3.2 in a near-back-scattering geometry, were superimposed one upon the other, following a procedure described elsewhere [25], in order to obtain composite spectra extending from 1 GHz to 5 THz. They are represented in figure 7(a) as susceptibility spectra, $\chi''(\omega) = I(\omega)/(n(\omega) + 1)$, where $n(\omega)$ is the Bose–Einstein factor. Such spectra are quite different from the DLS spectra recently obtained from several fragile glass-forming materials in two aspects. First, there is no sharp maximum on the low-frequency side, the frequency of this maximum having been identified in the other cases by its position and its temperature variation as the signature of the α process. Second, the minimum between the low-frequency side and the high-frequency spectrum (the latter being usually attributed to microscopic motions and also to the boson peak) is very shallow; its position becomes poorly defined as the temperature decreases. It has been pointed out in another case [41] that these spectra and their thermal evolution are very similar to what is measured in coherent inelastic neutron-scattering experiments. We tested this point by comparing our spectra with time-of-flight (TOF) spectra measured by Frick *et al* [8]. On fixing the relative intensity scale by imposing a common value between 0.1 meV$< E <$ 1 meV for DLS spectra at 233 K and TOF spectra at 240 K, figure 7(a) shows that, again, these spectra are very similar in the region where they overlap. The absence of the microscopic peak in the TOF spectra is only due to the subtraction procedure for this peak introduced in the data treatment of Frick *et al*. The DLS data, together with two different neutron-scattering data sets for which the subtraction procedure was not used, are shown in figure 7(b). It can be seen that, as already noticed by Sokolov *et al* [19], the relaxational part is the dominant part of these spectra below 1.5 meV.

The MCT analysis of the susceptibility spectra in the vicinity of the minimum is practically impossible because the minimum is very shallow and a much broader frequency

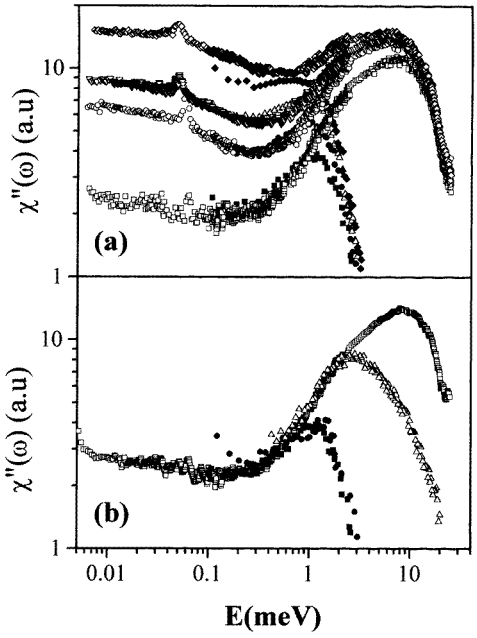

Figure 7. A comparison between composite and neutron susceptibility spectra. (a) Depolarized light scattering ((□), 213 K; (○), 233 K; (▽), 253 K and (◊), 273 K) and coherent neutron scattering [8] ((■), 220 K; (●), 240 K; (△), 260 K; and (♦), 280 K. The data from depolarized light scattering are multiplied by the same scaling factor, namely 3×10^{-2}. (b) Depolarized light scattering ((□), 213 K); coherent and incoherent neutron scattering [8, 19] ((■) and (●), 220 K; (△), 211 K).

range would be required, in contrast to those used in other studies, to characterize the limiting slopes a and b, if any, and to determine whether they would verify the relations predicted by the asymptotic expansions of MCT. Thus the power-law behaviour of the position of the minimum cannot be checked, because this position cannot be determined with any reasonable accuracy from the experimental data. The only test which can be reasonably carried out concerns the predicted power-law behaviour of the amplitude of the susceptibility in the frequency range of the expected minimum. Several sets of data for the amplitude of the susceptibility minimum obtained by coherent and incoherent neutron scattering [8, 19] are shown in figure 8, together with our own results. One can see that our results are in reasonable agreement with the previous data. Concerning our data, one can see in the inset of figure 8 that the amplitude of the susceptibility minimum is rather better represented by a law linear in temperature than it is by a $(T-T_c)^{1/2}$ law with $T_c = 216$ K [9]. Our DLS susceptibility data thus cannot be easily compared with the MCT susceptibilities. On the other hand, in the 3–300 GHz region, they reveal, as do the TOF results, a rather flat spectrum, the intensity of which increases linearly from $T = 200$ K to $T = 300$ K. The process contributing to this flat spectrum, being within the frequency range of the Brillouin line, clearly could interact with the longitudinal phonons and we must examine whether it was the large intensity of this relaxation channel which made it difficult to reconcile the Brillouin measurements with the NSE results.

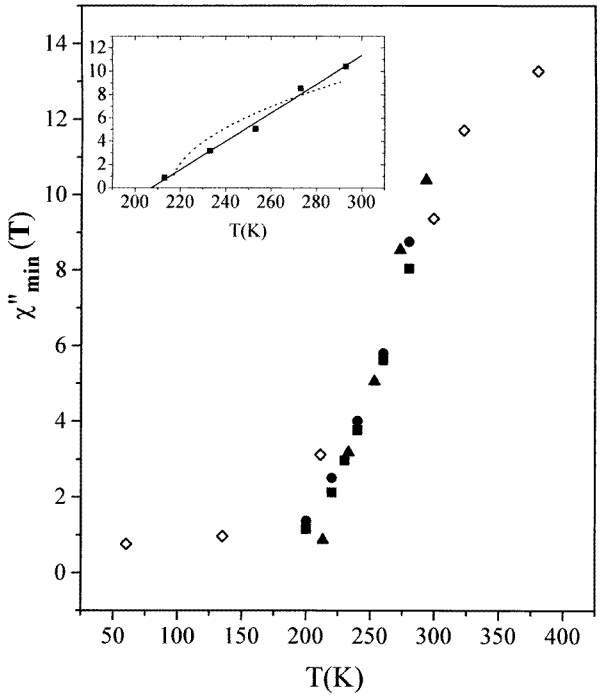

Figure 8. The temperature dependence of the minimum of the neutron scattering [8, 19] ((■), (●) and (△)) and DLS (□) susceptibilities. The inset shows the DLS minimum of the susceptibility (■), the linear approximation (——) and the $(T - T_c)^{1/2}$ law with $T_c = 216$ K [9] (– – –).

3.3. A further comparison of NSE and Brillouin relaxation times

The NSE measurements were interpreted by assuming that the density fluctuations they probe relax with a stretched exponential dynamics and equation (3) postulates that the long-wavelength phonons relax mostly through their coupling to these density fluctuations. This was the rationale for taking at first, in the $m(\omega)$ term, the same β as measured by NSE [9], adding a weak γ_0 effect for the high-frequency dynamics. Because we have just seen in the DLS spectra the existence of a flat feature, the intensity of which increases with temperature, one can wonder whether some proper description of that part of the spectrum would not be sufficient to reconcile the NSE and Brillouin results.

One possibility is that this flat spectrum is the sum of the α process and of the low-frequency tail of a fast relaxation process related, for instance, to the boson peak, which could be part of the high-frequency spectrum seen in figures 7(a) and (b). Such an idea has been proposed, for instance, by Loheider *et al* [42], to explain the Brillouin spectrum of the glass former $GeSBr_2$. Because our experiment would only be sensitive to the low-frequency tail of such a relaxation process, the latter can be simply represented by an $i\omega\gamma_0$ term, the corresponding real part, proportional to $(\omega\tau)^2$ giving a negligible contribution to the spectrum.

We thus tried a fit (fit 2) in which β and τ were taken at each temperature as the values measured in the NSE experiment, allowing γ_0 to vary freely. One sees in figure 3(b) that such a model gives quite acceptable fits in the vicinity of room temperature, where the NSE

τ_{KWW} values and the values of our initial fit are close. Conversely, at low temperature, the model cannot reproduce the 2–5 GHz part of the spectrum: the NSE τ_{KWW} values are too long to be able to reproduce the secondary rise in our spectra at low frequencies and the corresponding coefficients of the fit χ^2 are much higher than those in our initial analysis for the same number of free parameters.

This negative result suggests another possibility: as already mentioned, our DLS spectra did not detect the maximum of the α relaxation process, which could mean that the light-scattering probe detects this process only at lower frequencies; it should then just be sensitive to its high-frequency tail, the consequence of which could be both the high level of the DLS spectrum and the low-frequency increase in the Brillouin spectrum. Because fit 2 gave results as good as those of fit 1 at room temperature, we tried a third fit (fit 3) by fixing τ_{KWW} again to the neutron values at each temperature and γ_0 to the same as in fit 1 but letting β vary freely, to mimic this high-frequency tail. The results, shown in figure 3(c), though better than those in fit 2, follow the same trend: they cease to describe the low-frequency rise at low temperature while giving very low values for β ($\beta_{CD} < 0.2$). Those values are totally unreasonable for the α relaxation and still smaller than the β seen in the neutron experiment.

Nevertheless, let us notice that, although fits 2 and 3 yield a good description of the broadening of the Brillouin lines, neither of them can describe the low-frequency behaviour of the spectra at low temperature. Since the coupling parameter Δ was also a free fitting parameter in our three fits, variation in the coupling can result in a good fit of the phonon lines although this variation cannot take into account the behaviour of the central line. None of those two attempts was thus able to give a coherent description of the low-frequency part of our Brillouin spectra.

Combining the features of fits 2 and 3 could perhaps result in a satisfactory fit but in this case we would have to free one more parameter without any control. Insofar as the obvious implication of such a fit would be that there exists some supplementary contribution to the relaxation in the Brillouin region, different from the α relaxation, and because that is exactly our conclusion, we feel that this fit would not add much new insight into the problem. We are therefore led to conclude that the relaxation times seen by Brillouin scattering are different by one to two orders of magnitudes from those seen in the $q = 1.88$ Å^{-1} NSE experiment at low temperature.

4. The origin of the Brillouin relaxation mechanism

The preceding discussion has made it clear that the acoustic phonons couple to a relaxation mechanism which takes place on the nanosecond time scale (from 10^{-2} ns at 300 K to 1 ns at 200 K) and which apparently follows an Arrhénius law throughout the temperature range. A possible clue for the origin of the fast process which dominates our Brillouin spectra might be found in the recent work of Boyd *et al* [21]. Those authors followed the chain dynamics of *cis* and *trans* 1-4 polybutadiene samples through a molecular dynamics simulation method and analysed their results in terms of conformational changes of series of four successive atoms, focusing on the series which have a single bond as the middle bond. The conformation of the chain portion is defined as the angle between the two planes each of which contain the middle bond and a third carbon atom. This conformation is discretized by letting this angle have only three values, differing one from another by 120°. They further defined α bonds, for which one of the non-central bonds is a double bond, and β bonds, which have α bonds as non-central bonds, and they noted their non-symmetrical geometry, the former having a *cis* configuration when the four carbon atoms

are coplanar, whereas the latter have a *trans* configuration in the same case. Finally, they assumed potential barriers of approximately 2 and 3 kcal mol^{-1}, respectively. They found that linking the bonds together in a *cis* (or a *trans*) 1-4 chain and letting them interact with the neighbouring chains hardly affected this dynamics in the sense that the torsional dynamics of the α (respectively β) bonds interacting in the polymer, discretized as explained above, kept its individual activation energy, the number of torsional changes per bond being in the range of 10^{11} s^{-1} at 300 K.

From a general point of view, longitudinal phonons may be damped by any process whose frequency is in the same frequency range and which furthermore involves a length scale shorter than the phonon wavelength and a deformation which couples with these phonons. We suggest that the α bond torsional dynamics is the main motion which couples to the acoustic phonons and that this dynamics is responsible for their attenuation, through the following mechanism. Let us imagine that two successive double bonds are aligned along some direction x and that the three bonds which link those double bonds belong to the plane formed by the double bonds, as shown in figure 9(a), the two α bonds being in the *cis* configuration and the β bond in a *trans* configuration. The distance between the two double bonds along the x direction will be shorter than that when the β bond leaves this plane, the two α bonds being now in a *gauche* configuration (figure 9(b)). Such a change in length will probably be favoured by an acoustic phonon which locally increases that mean length between the atoms in the direction of the wavevector. This mechanism thus creates some coupling between the acoustic mode propagation and the conformational changes, clearly making available a damping channel for the phonon energy which will be transferred to the bond in order to allow the system to pass over the potential barrier. Moreover, because this change in length scale increases the local density, it is thus detected in the isotropic spectrum. The coupling of this torsional dynamics with the acoustic phonons will decrease with increasing value of the wavevector because this dynamics involves the relative position of six or more successive carbon atoms in the chain. Therefore, the coupling between the two dynamics will become inefficient when the phonon wavelength will be typically of the order of 3–3.5 Å. Experiments probing the carbon motions on such a short range will necessarily be sensitive to one of the many other aspects of the chain dynamics.

The preceding torsional dynamics results in density fluctuations which can be seen in the isotropic spectrum. Let us also remark that, although such dynamics could in principle be detected in the anisotropic spectrum also, it turns out that their coupling to the anisotropic part of the polarizability tensor is too weak to give rise to a significant signal. Indeed, the α bond torsional dynamics ends up changing the position of a CH_2 group belonging to a β bond; it thus modifies slightly the dielectric tensors both of this CH_2 group and of the nearby CH_2 and CH groups belonging to neighbour chains. Such local changes in the dielectric tensors modify their direction but this effect is small. It is likely that the torsional dynamics is at the origin of part of the low-frequency anisotropic spectrum, but the persistence, seen in figure 7, of a broad feature in the 5 GHz region down to 1 GHz indicates that the torsional dynamics is not the only source of the v–h spectra.

One weak point of the proposed mechanism for the acoustic wave attenuation is the value of the activation energy. From a calculation based on quantum chemistry, Boyd *et al* proposed, as already mentioned, a value of 2 kcal mol^{-1} for the α bond torsional dynamics. Our Brillouin measurements rather suggest a 4.8 kcal mol^{-1} value. However, figure 9(c) shows that the change of the β bond from configuration 1 (figure 9(a)) to configuration 2 (figure 9(b)) or 3 (not represented) modifies the length between the two neighbouring double bonds, whereas the change from configuration 2 to configuration 3 does not create such a modification. This means that the discrepancy in activation energies, besides the uncertainty

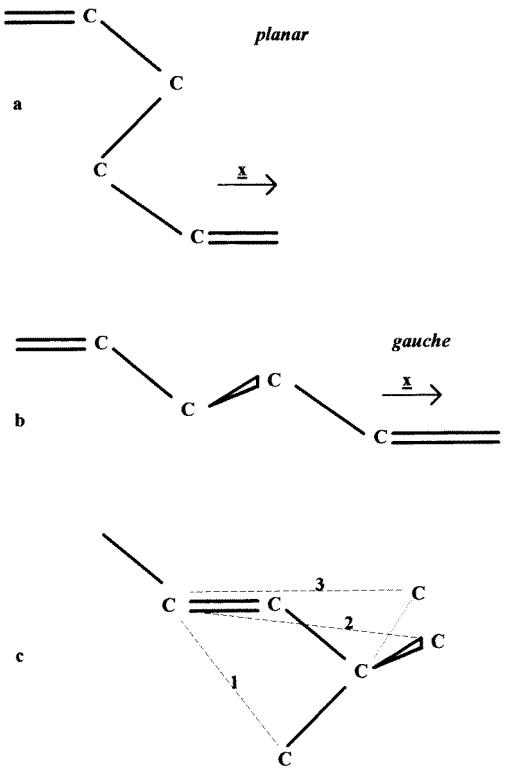

Figure 9. Configurations of four atoms: the distance between the two double bonds is shorter in the planar configuration (a) than it is in the *gauche* configuration (b). In (c) the change from configuration 1 to configurations 2 and 3 corresponds to a change in the length between these double bonds, whereas the change from configuration 2 to configuration 3 does not.

from the fitting procedure, could also arise as already noticed from the selection of specific conformation changes by the light-scattering technique used here.

5. Conclusion

We have measured the polarized and depolarized light-scattering spectra of 1-4 polybutadiene samples of molecular weights 7675 and 20 000 in the back-scattering geometry and at a scattering angle of 90° using two different tandem Fabry–Pérot interferometers. We found that the damping of the longitudinal phonons cannot be attributed to the well-documented α relaxation in PB.

We conclude that this damping is due to a β process, the temperature dependence of which is found to follow an Arrhénius behaviour with an activation energy of 4.8 kcal mol^{-1}. The β relaxation process contributes predominantly to the isotropic spectra and is due to isotropic density fluctuations. This process cannot be identified in the depolarized spectra which therefore cannot be used to explain the phonon damping. To identify this β process with the β process found in neutron scattering results in very low β_{CD}. In this case using this neutron-scattering β process does not result in a satisfactory fit of the central peak observed in our Brillouin spectra.

We suggest that the isotropic density fluctuations contributing to this process can be related to torsional dynamics. That these mechanisms are not clearly distinguished in the anisotropic spectrum could arise either because they do not contribute or because they are merged with other processes.

Acknowledgments

We gratefully acknowledge the financial support of the bilateral cooperation Procope programme 94034. AP and WS acknowledge partial support from the Deutsche Forschungsgemeinschaft (SFB262) and the EU European Mobility Programme ERBCHRXCT-920009. We also acknowledge F Lauprètre, H Z Cummins, A Sokolov and E W Fischer for fruitful discussions and comments, and B Bonello, B Perrin and R Gohier for their help in acoustic measurements.

References

[1] Richert R and Blumen A 1995 *Disorder Effects on Relaxational Processes* ed R Richert and A Blumen (Berlin: Springer) p 193
Richter D, Dianoux A J, Petry W and Teixeira J 1989 *Dynamics of Disordered Materials* vol I (Berlin: Springer) p 287
Richter D, Dianoux A J, Petry W and Teixeira J 1993 *Physica* A **201**
[2] Götze W 1991 *Liquids, Freezing and the Glass Transition, Proc. Les Houches Summer School* ed J P Hansen *et al* (Amsterdam: North-Holland) p 287
Götze W and Sjögren L 1992 *Rep. Prog. Phys.* **55** 241
[3] Kob W and Anderson H C 1994 *Phys. Rev. Lett.* **73** 1376
Kob W and Anderson H C 1995 *Phys. Rev.* E **51** 4626
Kob W and Anderson H C 1995 *Phys. Rev.* E **52** 4134
[4] Angell C A 1984 *Relaxation in Complex Systems* ed K L Ngai and G B Wright (Washington: NRL) p 3
[5] Fytas G and Meier G 1993 *Dynamic Light Scattering* ed W Brown (Oxford: Oxford University Press) p 403
[6] Frick B, Richter D, Petry W and Buchenau U 1988 *Z. Phys.* B **70** 73
[7] Frick B, Farago B and Richter D 1990 *Phys. Rev. Lett.* **64** 2921
[8] Frick B, Zorn R, Richter D and Farago B 1991 *J. Non-Cryst. Solids* **131** 169
[9] Richter D, Frick B and Farago B 1988 *Phys. Rev. Lett.* **61** 2465
[10] Richter D, Zorn R, Frick B, Fetters L J and Farago B 1992 *Phys. Rev. Lett.* **68** 71
[11] Richter D, Frick B and Ritter C 1989 *Europhys. Lett.* **9** 557
[12] Richter D, Zorn R, Frick B, Kremer F, Kirst U and Fetters J 1990 *Physica* B **180** 534
[13] Zorn R, Arbe A, Colmenero J, Frick B, Richter D and Buchenau U 1995 *Phys. Rev.* E **52** 781
[14] Arbe A, Buchenau U, Willner L, Richter D, Farago B and Colmenero J 1996 *Phys. Rev. Lett.* **76** 1872
Arbe A, Richter D, Colmenero J and Farago B 1997 submitted
[15] Hofmann A, Alegria A, Colmenero J, Willner L, Buscaglia E and Hadjichristidis N 1997 *J. Am. Chem. Soc.* at press
[16] Dejean de la Batie R, Lauprètre F and Monnerie L 1989 *Macromolecules* **22** 122
[17] Rössler E, Sokolov A P, Eiermann P and Warschewske U 1993 *Physica* A **202** 23
[18] Fioretto D, Palmieri L, Socino G and Verdini L 1994 *Phys. Rev.* B **50** 605
[19] Sokolov A P, Buchenau U, Steffen W, Frick B and Wischnewski A 1995 *Phys. Rev.* B **52** 9815
[20] Adolf D B and Ediger M D 1991 *Macromolecules* **24** 5834
[21] Gee R H and Boyd R H 1994 *J. Chem. Phys.* **101** 8028
[22] Kim E-G and Mattice W L 1994 *J. Chem. Phys.* **101** 6242
[23] Zorn R, McKenne G B, Willner C and Richter D 1995 *Macromolecules* **28** 8552
[24] Reinhardt L, Fischer E W and Fytas G 1996 *Acta Polymerica* **47** 399
[25] Lebon M J, Dreyfus C, Li G, Aouadi A, Cummins H Z and Pick R M 1995 *Phys. Rev.* E **51** 4537
[26] Steffen W, Patkowski A, Gläser H, Meier G and Fischer E W 1994 *Phys. Rev.* E **49** 2992
[27] Berne B and Pecora R 1976 *Dynamic Light Scattering* (New York: Wiley)
[28] Li G, Du W M, Chen X K, Cummins H Z and Tao N J 1992 *Phys. Rev.* A **45** 3867
[29] Tao N J, Li G and Cummins H Z 1992 *Phys. Rev.* B **45** 686

[30] Havriliak S and Negami S 1967 *Polymer* **8** 161
[31] Lindsay C P and Patterson G D 1980 *J. Chem. Phys.* **73** 3348
[32] Williams G and Watts D C 1970 *Trans. Faraday Soc.* **66** 80
Williams G, Watts D C, Dev S B and North A 1971 *Trans. Faraday Soc.* **67** 1323
Kohlrausch R 1947 *Pogg. Ann.* **12** 393
[33] Dreyfus C, Lebon M J, Cummins H Z, Toulouse J, Bonello B and Pick R M 1992 *Phys. Rev. Lett.* **69** 3666
[34] Li G, Du W M, Hernandez J and Cummins H Z 1993 *Phys. Rev.* E **48** 1192
[35] Fuchs M, Götze W and Latz A 1990 *Chem. Phys.* **149** 185
[36] Litovitz T A and Davis C M 1965 *Physical Acoustics* vol II part A ed W P Mason (London: Academic) p 281
[37] Rufflé B 1996 *Thesis* Rennes
[38] Viovy J L, Monnerie L and Merola F 1985 *Macromolecules* **18** 1130
[39] Campbell I A, Flesselles J M, Jullien R and Botet R 1988 *Phys. Rev.* B **37** 3825
[40] A forthcoming paper of Arbe A, Richter D, Colmenero J and Farago B [14] proposes a method to unify NSE and dielectric β-relation processes
[41] Wuttke J, Hernandez J, Li G, Coddens G, Cummins H Z, Fujara F, Petry W and Sillescu H 1993 *Phys. Rev. Lett.* **72** 3052
[42] Loheider S, Vögler G, Petscherizin I, Soltwisch M and Quitmann D 1990 *J. Chem. Phys.* **93** 5436